

Extraction of SUSY Parameters from Collider Data

Dirk Zerwas

LAL, Univ. Paris-Sud, CNRS/IN2P3, Orsay, France

Abstract.

The extraction of the parameters of the supersymmetric Lagrangian from collider data is discussed. Particular emphasis is put on the rigorous treatment of experimental and theoretical errors. While the LHC can provide a first estimate of the parameters, the combination of LHC and ILC will be necessary to determine with high precision the parameters of the MSSM.

Keywords: supersymmetry, Supersymmetric Models

PACS: 11.30.Pb, 12.60.Jv

INTRODUCTION

Supersymmetry with R-parity conservation is an attractive extension of the standard model. It predicts a light Higgs boson mass in agreement with the electroweak precision data, and provides a candidate for dark matter, the lightest neutralino. Moreover it provides the path to grand unification near the Planck scale.

Among the various models presently being studied, two stand out: mSUGRA as an example of a model with few parameters defined at the GUT scale and the MSSM with many parameters which is defined at the electroweak scale. The supersymmetric particles are produced in pairs, (cascade-) decaying to the lightest supersymmetric particle (LSP), most naturally the lightest neutralino. The characteristic signature is missing transverse energy.

In the following sections first the potential measurements at colliders, the LHC, the proton-proton collider with a center-of-mass energy of 14 TeV, and the ILC an e^+e^- linear collider with a center-of-mass energy of up to 1 TeV, will be discussed. Then the reconstruction of the fundamental parameters will be described. The results are summarized in the last section.

MEASUREMENTS

Supersymmetry can lead to a wealth of different signatures at colliders. To enable comparisons between experiments and/or colliders sets of parameters are defined to represent typical signatures. Most commonly known is the point SPS1a [1] which has been studied in detail in [2]. Points with similar phenomenology have been studied in ATLAS (SU3) and CMS (LM1 [3]). A summary of the points is shown in Table 1. In the following SPS1a will be studied as an example. The parameters of this point lead to squarks with masses of the or-

TABLE 1. Summary of mSUGRA parameter sets with similar collider phenomenology. μ is positive for all cases.

	SPS1a	SPS1a'	SU3	LM1
m_0	100	70	100	60
$m_{1/2}$	250	250	300	250
$\tan\beta$	10	10	6	10
A_0	-100	-300	-300	0

der of 500 GeV/ c^2 , light sleptons (150-200 GeV/ c^2) and the lightest Higgs boson mass being compatible with the LEP bound.

An important aspect of collider phenomenology at the LHC are long decay chains such

$$\tilde{q}_L \rightarrow \chi_2^0 q \rightarrow \tilde{\ell}_R \ell q \rightarrow \ell \ell q \chi_1^0. \quad (1)$$

The final state therefore contains at least a hard jet and two opposite sign same flavor leptons, where at the LHC lepton usually is restricted to be an electron or muon. In this decay chain five edges and thresholds can be calculated and reconstructed [2]. The expressions for these depend only on the four intervening masses. Therefore as the system is overdetermined the masses can be reconstructed, either via toy MC or fitting, without the use of assumptions on the underlying theory. Further signatures, e.g. the squark-R and the sbottoms, provide a total of 14 observable and measurable particles at the LHC. Typically the systematic error on measurements at the LHC coming from the jet energy scale is 1% and 0.1% for the lepton energy scale. With integrated luminosities of up to 300 fb $^{-1}$ the statistical error in many cases is smaller than the systematic error.

The scenario of SPS1a has been analyzed to great detail, providing to this day the benchmark point for studies at the ILC and LHC. More recent studies have increased the robustness of the results. The experiments have moved from fast simulations to full simulation and

reconstruction This includes the detailed description of detectors as shown at this conference [4, 5, 6].

While the determination of masses at the LHC can be performed most accurately by analyzing long decay chains, the ILC can measure, either via threshold scans or direct reconstruction the masses of essentially all kinematically accessible particles. This typically leads to a precision at the permil level. As the LSP mass is measured more precisely at the ILC than at the LHC, one can insert the ILC measured LSP mass into the mass determination at the LHC thus reducing the error on the squark mass measurement as shown in [7].

RECONSTRUCTING THE FUNDAMENTAL PARAMETERS

Collider measurements are sensitive to several parameters and different observables depend on different combinations of the fundamental parameters. The system to be solved is therefore strongly correlated. A global Ansatz to make use of all information in an optimal way is therefore necessary.

Precise theoretical predictions are necessary in order to reconstruct the parameters. The ingredients [8] for such an endeavor, without attempting to be complete, are: precise mass calculations by SuSpect, SOFT-SUSY and SPheno [9, 10, 11]. Branching ratios are provided by SUSY-Hit which includes SDecay for the decay of supersymmetric particles and HDecay for the decays of the Higgs bosons [12, 13, 14]. e^+e^- cross sections are calculated by PYTHIA and SPheno [15, 11], while NLO proton–proton cross sections are provided by Prospino2.0 [16, 17, 18, 19].

To extract the parameters, the experimental data are analyzed by making use of these individual packages with a proper treatment of statistical, experimental systematic and theoretical errors. Pioneering work on parameter extraction with upward running to the GUT scale was done in [7, 20]. The Fittino [21] group and the SFitter collaboration [22] have worked on methods for the search for minima and the proper extraction of errors. More recently GFitter has presented a new package for the electroweak fit. The package Super-Bayes originated in the study of the dark matter aspect of supersymmetry [23].

The standard model electroweak measurements with the addition of the WMAP [24] measurement of the relic density already allows to delimit interesting regions of parameter space without the direct observation of supersymmetric particles. In particular as shown in [25, 26], the supersymmetric fit of mSUGRA results in a prediction for the lightest Higgs boson mass of $m_h = 110^{+8}_{-10} \pm 3 \text{ GeV}/c^2$, pushing the Higgs boson mass closer, with

TABLE 2. List of the best log–likelihood values over the mSUGRA parameter space using only the LHC measurements [22].

χ^2	m_0	$m_{1/2}$	$\tan\beta$	A_0	μ	m_t
0.09	102.0	254.0	11.5	-95.2	+	172.4
1.50	104.8	242.1	12.9	-174.4	–	172.3
73.2	108.1	266.4	14.6	742.4	+	173.7
139.5	112.1	261.0	18.0	632.6	–	173.0

respect to the standard model fit, to the limit of direct searches at LEP of $114.4 \text{ GeV}/c^2$ [27]. The distribution of the allowed cross sections for supersymmetric particles at the LHC was shown in [28].

mSUGRA parameter determination

Under the hypothesis that supersymmetric particles have been discovered and measured at the LHC and ILC and their discrete quantum numbers (e.g. spin) have been determined, there are two separate issues in the actual determination of parameters that need to be addressed:

1. Can the correct SUSY parameter set be found?
2. What is the precision of the determination of the parameters?

mSUGRA provides a good testing ground for studying the techniques to answer these questions. The disadvantage of mSUGRA is that it starts with universal parameters at the GUT scale, adds the RGE-extrapolation to the weak scale, and that it is not the most general Lagrangian.

To address the first question, SFitter performed 300 toy experiments where the starting point of the simple MINUIT [29] fit was far away from the true values. The fits converged to the true values of SPS1a already for the case where only LHC measurements, thus those with the largest errors, are available.

Beyond the simple fit, powerful algorithms have been developed to sample multi-parameter space: The Fittino group has implemented simulated annealing which allows to escape out of secondary minima where a simple fit would have been confined to a wrong parameter subspace. SFitter uses weighted Markov chains which allow for an efficient sampling of high dimensional parameter space. A full dimensional exclusive likelihood map is produced with the possibility of different kinds of projection: marginalization (the Bayesian approach) or the profile likelihood (frequentist approach). Markov chains are also able to identify secondary minima. The computing intensive method of dividing the parameters into a grid has also been implemented.

The two-dimensional profile likelihood in the m_0 – $m_{1/2}$ plane is shown as an example in Figure 1. The

TABLE 3. Best-fit results and errors for mSUGRA at the LHC (endpoints) and including ILC measurements taken from [22].

	SPS1a	$\Delta_{\text{endpoints}}$	Δ_{ILC}	$\Delta_{\text{LHC+ILC}}$	$\Delta_{\text{endpoints}}$	Δ_{ILC}	$\Delta_{\text{LHC+ILC}}$
		exp. errors			exp. and theo. errors		
m_0	100	0.50	0.18	0.13	2.17	0.71	0.58
$m_{1/2}$	250	0.73	0.14	0.11	2.64	0.66	0.59
$\tan\beta$	10	0.65	0.14	0.14	2.45	0.35	0.34
A_0	-100	21.2	5.8	5.2	49.6	12.0	11.3
m_t	171.4	0.26	0.12	0.12	0.97	0.12	0.12

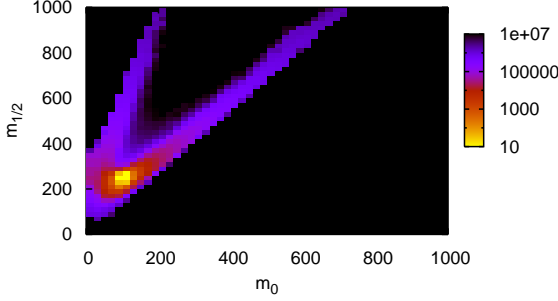


FIGURE 1. SFitter output for mSUGRA in SPS1a. Two-dimensional profile likelihood χ^2 over the m_0 - $m_{1/2}$ plane using only the LHC measurements.

minimum at the correct nominal values is clearly visible. The search for secondary minima is illustrated in Table 2. Indeed, even in mSUGRA alternative minima can be found. It is interesting to note that the third minimum results from the interplay of the A_0 parameter and the top quark mass (measurement error 1 GeV/c²). This illustrates the necessity to take into account not only the supersymmetric measurements, but also the standard model parameters as part of the parameter sets. It is also a tale of caution: while the secondary minima can be discarded easily in this case by using the χ^2 value, it is obvious that the unambiguous identification of the correct parameter set will become more complex in the MSSM case.

To determine the correct errors on the parameters, not only experimental errors, but also the theoretical uncertainties, e.g. on the mass calculations, have to be taken into account. The RFit scheme [30]:

$$\chi_{d,i} = 0 \quad |d_i - \bar{d}_i| < \sigma_i^{(\text{theo})} \quad (2)$$

$$\chi_{d,i} = \frac{|d_i - \bar{d}_i| - \sigma_i^{(\text{theo})}}{\sigma_i^{(\text{exp})}} \quad |d_i - \bar{d}_i| > \sigma_i^{(\text{theo})} \quad (3)$$

defines the χ^2 contribution as zero within the range of the theoretical error. This is appropriate as the theoretical errors are non-Gaussian. This treatment insures that no

parameter value within the theory errors is privileged. Typical values for the theoretical precision are 3 GeV/c² on the Higgs boson mass [31], 1% on the masses of non-colored particles and 3% on the masses of strongly interacting particles [22].

Based on the mass determination at the LHC, the fundamental parameters can be determined with a precision at the percent level. Using the edges instead of the masses, thus using the experimental observables directly, the precision is improved by a factor 3 to 8. When calculating the masses from the edges, correlations among masses are introduced, as these are not available, the results differ. A second remark is that using the correlation of the experimental systematic errors (energy scale) influences the error at the level of 25% to 50%. Thus it will be important for the experiments to control these correlations with good precision. The best strategy to determine the parameters is to start from the experimental measurements and not intermediate quantities.

Once the ILC becomes operational, the emphasis will turn even more to the precision determination of the parameters. The result of the error determination for the LHC, ILC and their combination is shown in Table 3. In general the ILC improves the precision by almost an order of magnitude and the combination of the two machines is more powerful than any single one. In particular the measurement of $\tan\beta$ is improved as the neutralino/chargino sector is completely measured and the heavy Higgs bosons are within the kinematic reach of the ILC and can therefore be measured with high precision. Including theoretical errors does not change this picture. However it is interesting to note that they cannot even be neglected at the LHC alone. Therefore it is important already for the LHC to improve the precision of the theoretical predictions. The SPA convention and project [32] provides a framework for this work.

An interesting topic to illustrate that the determination of parameters will be an iterative process (even for mSUGRA), is the neutralino enigma at the LHC. The LHC will be able to measure three neutralinos, therefore there is an ambiguity as to which ones: $\chi_1^0, \chi_2^0, \chi_3^0$ or $\chi_1^0, \chi_2^0, \chi_4^0$ or $\chi_1^0, \chi_3^0, \chi_4^0$? The last combination can be ruled out easily by the χ^2 of the fit. However the first

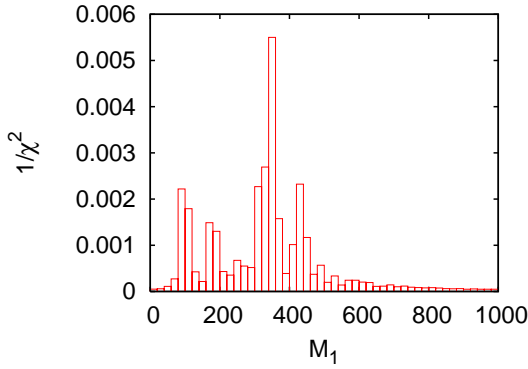


FIGURE 2. Profile likelihood for the neutralino sector from SFitter taken from [22].

two combinations both give a rather reasonable χ^2 . m_0 and $m_{1/2}$ are correctly determined, only $\tan\beta$ and A_0 are off, but they are not measured very precisely. However, the pre-determined parameters can be used to predict the mass and the branching ratio of the missing neutralino. As more χ_4^0 are predicted than χ_3^0 , the LHC alone can iteratively solve this problem.

MSSM and extrapolation to the high scale

The MSSM is more complex to analyze than mSUGRA as there are many more parameters to be determined. Typically 19 parameters are to be measured in the MSSM. In such a difficult environment not one single technique of finding the right parameter set but a mix is necessary. Taking the SFitter analysis as an example: a multi-step procedure of Markov chains alternating with MINUIT is used to analyze the MSSM.

Three neutralino masses and no chargino masses are measured at the LHC in the point SPS1a. This results in a 8-fold ambiguity in gaugino-Higgsino subspace. The χ^2 values in these points are essentially degenerate. Figure 2 shows the distribution of the inverse χ^2 for M_1 . Four peaks are clearly seen. They correspond to the central values of the eight solutions. The solutions for positive and negative μ are too close to be distinguished in the Figure.

When the ILC measurements are added, all parameters can be determined. Moreover, the precision of the measurement of the parameters is improved. The results of the error determination of the LHC and ILC individually as well the combination of the two is shown in Table 4 including flat theory errors.

Having determined the MSSM parameters at the electroweak scale, the natural extension of the analysis (in contrast to mSUGRA) is the evolution of the parameters to the GUT scale as shown in [20, 21, 22]. An example is

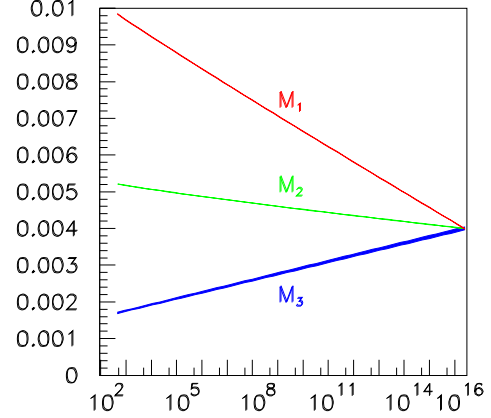


FIGURE 3. The upward renormalization group running of the inverse of the three gaugino masses in the MSSM as function of the energy scale in GeV [7, 20, 21].

shown in Figure 3 for the inverse of the gaugino mass parameters. As expected the three parameters unify similar to the unification of the gauge coupling constants at the GUT scale (10^{16} GeV). This observation holds true also for the unification of the mass parameters in the sfermion sector as well as the tri-linear couplings. Thus by measuring the MSSM parameters at the electroweak scale, a window is opened to study the physics scenario at the Planck scale.

SUSY with heavy scalars

The point SPS1a is a parameter set favorable for both the LHC and ILC. However even in difficult scenarios such as Split-SUSY [33, 34, 35] (or SUSY with heavy scalars [36]) parameters of the underlying theory can be determined.

The following scenario has been studied [37, 38]: the scalar mass scale is set to at least 10^4 GeV/ c^2 , thus the scalars are out of reach at colliders. The neutralinos and charginos have masses less than a TeV/ c^2 . In the Higgs sector only the lightest Higgs boson is observable.

The parameters to be determined are: μ the Higgs mass parameter, $\tan\beta$ the mixing angle in the Higgs sector at the scalar mass scale, the gaugino mass parameters and the tri-linear coupling at the scalar mass scale. The scalar mass scale is fixed in this analysis.

While the standard long decay chain is not available as the squarks are too heavy, the gaugino sector provides additional observables. The tri-lepton signal from the production and decay of the lightest chargino and the next-to-lightest neutralino provide information on the mass difference between the χ_2^0 and χ_1^0 . Abundant production of gluinos is observed, and the cross section is used in the fit.

TABLE 4. Results for the general MSSM parameter determination in SPS1a assuming flat theory errors. As experimental measurements the kinematic endpoint measurements are used for the LHC column, and the mass measurements for the ILC column. In the LHC+ILC column these two measurements sets are combined. Shown are the nominal parameter values and the result after fits to the different data sets. All masses are given in GeV [22].

	LHC		ILC		LHC+ILC		SPS1a
$\tan\beta$	10.0 \pm 4.5		13.4 \pm 6.8		12.3 \pm 5.3		10.0
M_1	102.1 \pm 7.8		103.0 \pm 1.1		103.1 \pm 0.84		103.1
M_2	193.3 \pm 7.8		193.4 \pm 3.1		193.2 \pm 2.3		192.9
M_3	577.2 \pm 14.5		fixed 500		579.7 \pm 12.8		577.9
$M_{\tilde{t}_L}$	227.8 \pm (10 ³)		183.8 \pm 16.6		187.3 \pm 12.9		193.6
$M_{\tilde{t}_R}$	164.1 \pm (10 ³)		143.9 \pm 17.9		140.1 \pm 14.1		133.4
$M_{\tilde{b}_L}$	193.2 \pm 8.8		194.4 \pm 1.1		194.5 \pm 1.0		194.4
$M_{\tilde{b}_R}$	135.0 \pm 8.3		135.9 \pm 1.0		136.0 \pm 0.89		135.8
$M_{\tilde{e}_L}$	193.3 \pm 8.8		194.4 \pm 0.89		194.4 \pm 0.84		194.4
$M_{\tilde{e}_R}$	135.0 \pm 8.3		135.8 \pm 0.81		135.9 \pm 0.77		135.8
$M_{\tilde{q}^3_L}$	481.4 \pm 22.0		507.2 \pm (4 \cdot 10 ²)		486.6 \pm 19.5		480.8
$M_{\tilde{t}_R}$	415.8 \pm (10 ²)		440.0 \pm (4 \cdot 10 ²)		410.7 \pm 48.4		408.3
$M_{\tilde{b}_R}$	501.7 \pm 17.9		fixed 500		504.0 \pm 17.4		502.9
$M_{\tilde{q}_L}$	524.6 \pm 14.5		fixed 500		526.1 \pm 7.2		526.6
$M_{\tilde{q}_R}$	507.3 \pm 17.5		fixed 500		508.4 \pm 16.7		508.1
A_τ	fixed 0		633.2 \pm (10 ⁴)		139.6 \pm (10 ⁴)		-249.4
A_t	-509.1 \pm 86.7		-516.1 \pm (10 ³)		-500.1 \pm 143.4		-490.9
A_b	fixed 0		fixed 0		-686.2 \pm (10 ⁴)		-763.4
$A_{l1,2}$	fixed 0		fixed 0		fixed 0		-251.1
$A_{u1,2}$	fixed 0		fixed 0		fixed 0		-657.2
$A_{d1,2}$	fixed 0		fixed 0		fixed 0		-821.8
m_A	406.3 \pm (10 ³)		393.8 \pm 1.6		393.9 \pm 1.6		394.9
μ	350.5 \pm 14.5		343.7 \pm 3.1		354.8 \pm 2.8		353.7
m_t	171.4 \pm 1.0		171.4 \pm 0.12		171.4 \pm 0.12		171.4

In the limit of infinite statistics, but taking into account theory errors, $\tan\beta$ is undetermined. By contrast, other parameters could be measured with a precision of several percent. The theoretical error on the gluino cross section was taken to be 30%. It is interesting to note that if the error were negligible, the error on the gaugino mass would be improved by a factor 10. This shows the importance of precise theoretical calculations at the LHC.

Connection to cosmology

As demonstrated in [39] the connection between particle physics and cosmology can be established at the LHC and ILC. First determining the parameters of the Lagrangian via the collider data, the parameters can be used to calculate ([40, 41, 42]) the relic density Ωh^2 . Shown in Figure 4 is the probability density of the relic density for SPS1a' which differs from SPS1a only slightly as shown in Table 1. In this point m_0 and A_0 were adjusted in order to lower the relic density which is too large to be compatible with the WMAP measurements [24]. The improvement from the combination LHC+ILC is clearly

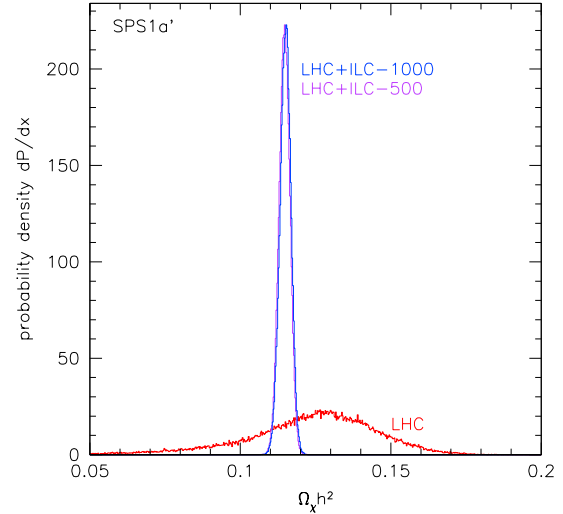


FIGURE 4. Probability density of the relic density Ωh^2 for SPS1a' for the LHC and the LHC+ILC [39].

visible.

At SPS1a in the mSUGRA scenario, neglecting the

theory errors, a precision of 3% can be expected from the LHC alone, with the ILC improving the precision by an order of magnitude. The precision is comparable to that of the futur Planck experiment (2% [43, 44]). The agreement between collider and cosmology measurements will be crucial to establish supersymmetry as the real solution to the dark matter enigma.

CONCLUSIONS

The LHC alone can provide a wealth of measurements for supersymmetry. The combination of LHC plus ILC is the optimal choice for the precision determination of all supersymmetric parameters at colliders, allowing a stable evolution of the theory near to the Planck scale. Once the parameters are determined it will be interesting to confront the prediction of the relic density from collider measurements with the measurements of WMAP and Planck. With the LHC starting this year, supersymmetry could be just around the corner.

ACKNOWLEDGMENTS

It was a pleasure to attend Supersymmetry 2008 in Seoul. I would like to thank Klaus Desch, Rémi Lafaye, Tilman Plehn, Michael Rauch, Laurent Serin, Mathias Uhlenbrock, Peter Wienemann and Peter Zerwas for help in preparing talk and manuscript. The manuscript was written in the stimulating atmosphere of the workshop “LHC: beyond the standard model signals in a QCD environment” at the Center of Physics in Aspen.

REFERENCES

1. B. C. Allanach, et al. (2002), hep-ph/0202233.
2. G. Weiglein, et al., *Phys. Rept.* **426**, 47–358 (2006), hep-ph/0410364.
3. G. L. Bayatian, et al., *J. Phys.* **G34**, 995–1579 (2007).
4. P. de Jong, *these proceedings*. (2008).
5. P. Wienemann, *these proceedings*. (2008).
6. C. Autermann, *these proceedings*. (2008).
7. G. A. Blair, W. Porod, and P. M. Zerwas, *Eur. Phys. J.* **C27**, 263–281 (2003), hep-ph/0210058.
8. B. C. Allanach (2008), 0805.2088.
9. A. Djouadi, J.-L. Kneur, and G. Moultaka, *Comput. Phys. Commun.* **176**, 426–455 (2007), hep-ph/0211331.
10. B. C. Allanach, *Comput. Phys. Commun.* **143**, 305–331 (2002), hep-ph/0104145.
11. W. Porod, *Comput. Phys. Commun.* **153**, 275–315 (2003), hep-ph/0301101.
12. M. Muhlleitner, A. Djouadi, and Y. Mambrini, *Comput. Phys. Commun.* **168**, 46–70 (2005), hep-ph/0311167.
13. A. Djouadi, M. M. Muhlleitner, and M. Spira, *Acta Phys. Polon.* **B38**, 635–644 (2007), hep-ph/0609292.
14. A. Djouadi, J. Kalinowski, and M. Spira, *Comput. Phys. Commun.* **108**, 56–74 (1998), hep-ph/9704448.
15. T. Sjostrand, S. Mrenna, and P. Skands, *JHEP* **05**, 026 (2006), hep-ph/0603175.
16. W. Beenakker, R. Hopker, M. Spira, and P. M. Zerwas, *Nucl. Phys.* **B492**, 51–103 (1997), hep-ph/9610490.
17. W. Beenakker, M. Kramer, T. Plehn, M. Spira, and P. M. Zerwas, *Nucl. Phys.* **B515**, 3–14 (1998), hep-ph/9710451.
18. W. Beenakker, et al., *Phys. Rev. Lett.* **83**, 3780–3783 (1999, Erratum-ibid.100:029901,2008), hep-ph/9906298.
19. T. Plehn (1998), hep-ph/9809319.
20. B. C. Allanach, et al. (2004), hep-ph/0403133.
21. P. Bechtle, K. Desch, W. Porod, and P. Wienemann, *Eur. Phys. J.* **C46**, 533–544 (2006), hep-ph/0511006.
22. R. Lafaye, T. Plehn, M. Rauch, and D. Zerwas, *Eur. Phys. J.* **C54**, 617–644 (2008), 0709.3985.
23. R. R. de Austri, R. Trotta, and L. Roszkowski, *JHEP* **05**, 002 (2006), hep-ph/0602028.
24. D. N. Spergel, et al., *Astrophys. J. Suppl.* **170**, 377 (2007), astro-ph/0603449.
25. S. Heinemeyer, *these proceedings*. (2008).
26. O. Buchmueller, et al., *Phys. Lett.* **B657**, 87–94 (2007), 0707.3447.
27. R. Barate, et al., *Phys. Lett.* **B565**, 61–75 (2003), hep-ex/0306033.
28. B. C. Allanach, K. Cranmer, C. G. Lester, and A. M. Weber, *JHEP* **08**, 023 (2007), 0705.0487.
29. F. James, and M. Roos, *Comput. Phys. Commun.* **10**, 343–367 (1975).
30. A. Hocker, H. Lacker, S. Laplace, and F. Le Diberder, *Eur. Phys. J.* **C21**, 225–259 (2001), hep-ph/0104062.
31. G. Degrossi, S. Heinemeyer, W. Hollik, P. Slavich, and G. Weiglein, *Eur. Phys. J.* **C28**, 133–143 (2003), hep-ph/0212020.
32. J. A. Aguilar-Saavedra, et al., *Eur. Phys. J.* **C46**, 43–60 (2006), hep-ph/0511344.
33. N. Arkani-Hamed, and S. Dimopoulos, *JHEP* **06**, 073 (2005), hep-th/0405159.
34. G. F. Giudice, and A. Romanino, *Nucl. Phys.* **B699**, 65–89 (2004 Erratum-ibid.B706:65-89,2005), hep-ph/0406088.
35. W. Kilian, T. Plehn, P. Richardson, and E. Schmidt, *Eur. Phys. J.* **C39**, 229–243 (2005), hep-ph/0408088.
36. N. Bernal, A. Djouadi, and P. Slavich, *JHEP* **07**, 016 (2007), 0705.1496.
37. E. Turlay (2008), 0805.2272.
38. M. M. Nojiri, et al. (2008), 0802.3672.
39. E. A. Baltz, M. Battaglia, M. E. Peskin, and T. Wizansky, *Phys. Rev.* **D74**, 103521 (2006), hep-ph/0602187.
40. P. Gondolo, et al., *JCAP* **0407**, 008 (2004), astro-ph/0406204.
41. G. Belanger, F. Boudjema, A. Pukhov, and A. Semenov (2008), 0803.2360.
42. G. Belanger, F. Boudjema, A. Pukhov, and A. Semenov, *Comput. Phys. Commun.* **176**, 367–382 (2007), hep-ph/0607059.
43. J. Lesgourgues, S. Prunet, and D. Polarski, *Mon. Not. Roy. Astron. Soc.* **303**, 45–49 (1999), astro-ph/9807020.
44. A. Balbi, C. Baccigalupi, F. Perrotta, S. Matarrese, and N. Vittorio, *Astrophys. J.* **588**, L5–L8 (2003), astro-ph/0301192.